






Article

Effect of Support Functionalization on Catalytic Direct Hydrogenation and Catalytic Transfer Hydrogenation of Muconic Acid to Adipic Acid

Elisa Zanella *, Stefano Franchi , Narmin Jabbarli, Ilaria Barlocco , Marta Stucchi  and Carlo Pirola *

Dipartimento di Chimica, Università degli Studi di Milano, Via Golgi 19, 20133 Milan, Italy; stefano.franchi@studenti.unimi.it (S.F.); narmin.jabbarli@unimi.it (N.J.); ilaria.barlocco@unimi.it (I.B.); marta.stucchi@unimi.it (M.S.)

* Correspondence: elisa.zanella@unimi.it (E.Z.); carlo.pirola@unimi.it (C.P.); Tel.: +39-02-5031-4283 (C.P.)

Abstract: The liquid-phase hydrogenation of muconic acid (MA) to produce bio-adipic acid (AdA) is a prominent environmentally friendly chemical process, that can be achieved through two distinct methodologies: catalytic direct hydrogenation using molecular hydrogen (H₂), or catalytic transfer hydrogenation utilizing a hydrogen donor. In this study, both approaches were explored, with formic acid (FA) selected as the hydrogen source for the latter method. Palladium-based catalysts were chosen for these processes. Metal's nanoparticles (NPs) were supported on high-temperature heat-treated carbon nanofibers (HHT-CNFs) due to their known ability to enhance the stability of this metal catalyst. To assess the impact of support functionalization on catalyst stability, the HHT-CNFs were further functionalized with phosphorus and oxygen to obtain HHT-P and HHT-O, respectively. In the hydrogenation reaction, catalysts supported on functionalized supports exhibited higher catalytic activity and stability compared to Pd/HHT, reaching an AdA yield of about 80% in less than 2 h in batch reactor. The hydrogen-transfer process also yielded promising results, particularly with the 1%Pd/HHT-P catalyst. This work highlights the efficacy of support functionalization in improving catalyst performance, particularly when formic acid is used as a safer and more cost-effective hydrogen donor in the hydrogen-transfer process.

Keywords: catalytic transfer hydrogenation (CTH); muconic acid; bio-adipic acid; formic acid; hydrogen donor; palladium catalysts; support functionalization



Citation: Zanella, E.; Franchi, S.; Jabbarli, N.; Barlocco, I.; Stucchi, M.; Pirola, C. Effect of Support Functionalization on Catalytic Direct Hydrogenation and Catalytic Transfer Hydrogenation of Muconic Acid to Adipic Acid. *Catalysts* **2024**, *14*, 465. <https://doi.org/10.3390/catal14070465>

Academic Editors: Leonarda Liotta and Shihui Zou

Received: 31 May 2024
Revised: 5 July 2024
Accepted: 16 July 2024
Published: 19 July 2024



Copyright: © 2024 by the authors. Licensee MDPI, Basel, Switzerland. This article is an open access article distributed under the terms and conditions of the Creative Commons Attribution (CC BY) license (<https://creativecommons.org/licenses/by/4.0/>).

1. Introduction

One of the greatest challenges facing the chemical industry in the 21st century is rethinking traditional processes in an environmentally responsible manner and transforming waste into valuable products. In this scenario, the nylon industry faces an enormous challenge since it plays a vital role in modern manufacturing due to the versatility and performance of nylon materials across a wide range of applications, such as textiles, automotive, packaging and carpets. One of the main production processes is the polymerization, where nylon is produced through the reaction between monomers, such as adipic acid and hexamethylene diamine to form nylon-6,6 [1]. The reaction yields a polymer that can be processed into fibers, films, or other forms. The production of nylon involves the use of petrochemicals and energy-intensive processes, which can contribute to greenhouse gases emissions and environmental pollution [2]. Indeed, adipic acid (AdA) is commercially produced by reducing benzene to cyclohexane, which is then oxidised to K-A oil, a mixture of cyclohexanol and cyclohexanone. In addition, the use of nitric acid to further oxidize this mixture to AdA accounts for 10% of artificial nitrous oxide production [3]. However, discontinuing the use of adipic acid is difficult. Efforts are underway to develop sustainable alternatives such as bio-based adipic acid derived from renewable resources

like waste woods [4]. Indeed, through biological processes from biomass, namely lignin [5] or cellulose [6], it is possible to obtain muconic acid that can be hydrogenated to adipic acid.

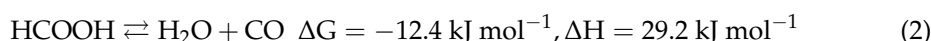
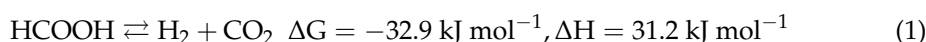
The liquid-phase hydrogenation of muconic acid to bio-adipic acid can be carried out via two distinct chemical processes: catalytic direct hydrogenation (CDH) using molecular hydrogen (H₂) gas or catalytic transfer hydrogenation (CTH) utilising a hydrogen donor. The second strategy employs chemicals such as hydrides (e.g., NaBH₄) [7], hydrazine hydrates [8] and organic reagents (e.g., alcohol, glycerol or formic acid) [9–12] as hydrogen donor in the hydrogenation process.

Heterogeneous catalytic transfer hydrogenation is a highly controlled process owing to the on-site production of hydrogen, eliminating the need for external hydrogen gas, which can be hazardous and requires specialized handling and equipment. Therefore, the minimal procedure risk, simplicity, cost-effectiveness, and durability and longevity of the catalyst make it a valuable strategy [13]. The challenges of this procedure are to identify the most effective metallic catalyst that offers high activity, selectivity and stability and to select the appropriate hydrogen sources that has to be efficient, cost-effective and compatible with the catalyst and substrate [14].

The solid catalyst facilitates the transfer of hydrogen from the donor to the substrate, typically involving metals such as palladium, nickel, or ruthenium supported on materials like carbon, silica, or alumina.

In this work, both processes CDH and CTH were considered and investigated. For the CTH process, formic acid (FA) has been used as a source of hydrogen. Indeed, the high volumetric capacity (53 g H₂/L), its liquid form and its low toxicity and low flammability under ambient conditions make formic acid a promising hydrogen carrier [15]. Furthermore, its decomposition can produce CO₂ as a by-product, which can be potentially recovered and reused for the synthesis of new chemical compounds, such as formic acid itself [16].

The formic acid decomposition (FAD) follows two different competing pathways: the first one (Equation (1)), in which hydrogen and carbon dioxide are produced, is the desired reaction, crucial for the storage of hydrogen; while the second reaction (Equation (2)), which generates CO and H₂O, is an undesirable side reaction due to the fact that CO can poison the active site of the catalysts, particularly in the case of platinum group metals [17–20].



Concerning the catalytic materials, for both FA decomposition and MA hydrogenation reactions are actually based on platinum group metals. In particular, among all, palladium in the form of supported nanoparticles (NPs) presents higher catalytic activity under mild conditions (e.g., temperature under 80 °C and ambient pressure) [21]. However, the main drawbacks of these metals are the low stability and selectivity [22]. A way to solve these problems can be the modification of the structure of the support, that has a great influence on the nature of the active phase greatly affecting the final performance of the catalyst [23]. In particular, a good interaction can enhance the stability of the catalyst preventing migration, coalescence, and Ostwald ripening phenomenon [24].

In this work, High-temperature Heat Treated Carbon Nanofibers (HHT-CNFs) were selected as support, since they are known to enhance the stability of palladium, in fact the formation of smaller and homogeneously dispersed Pd nanoparticles is favoured [25–27]. Carbon supports have also the great advantages to be cheap, stable and exceptionally versatile through modification of its structure, leading to the possibility of tune the electronic and geometric properties influencing the metal-support interaction and so the catalytic performance [28,29]. In particular, the introduction of heteroatoms, e.g., O, N, B and P, in the carbon structure can be a possible solution.

In this study, the bare HHT-CNFs were then functionalized with phosphorous and oxygen to obtain HHT-P and HHT-O, respectively, to study the effect of the support functionalisation. Using these supports, palladium-based catalysts with a metal loading

of 1% were synthesized, using sol immobilization technique [30]. The same systems were previously employed by our group in the study of the formic acid decomposition (FAD) reaction [31]. Indeed, an enhanced activity, stability and selectivity was observed for hydrogen production. Density functional theory (DFT) studies on the catalytic system showed that Pd cluster was stabilised on P- and O- functional groups decreasing the problem of the leaching of the metal.

Because of this improved stability and selectivity, it was decided to evaluate these catalysts in the hydrogenation of muconic acid and in the CTH process mediated by formic acid. The results are characterized by an enhancement of the catalytic performance following this order 1%Pd/HHT < 1%Pd/HHT-O < 1%Pd/HHT-P for both the process. The results obtained in the CTH process were also compared with those achieved in a previous study of our group [26], where PdRh based catalysts were tested in the MA hydrogenation reaction using formic acid as hydrogen donor. All the PdRh catalysts showed good activity for the first step of the reaction (Figure 1), however only using bimetallic catalysts the formation of adipic acid was enhanced. However, in the present work, it was found that also monometallic palladium, thanks to the functionalization of the support, can lead to the formation of bio-adipic acid.

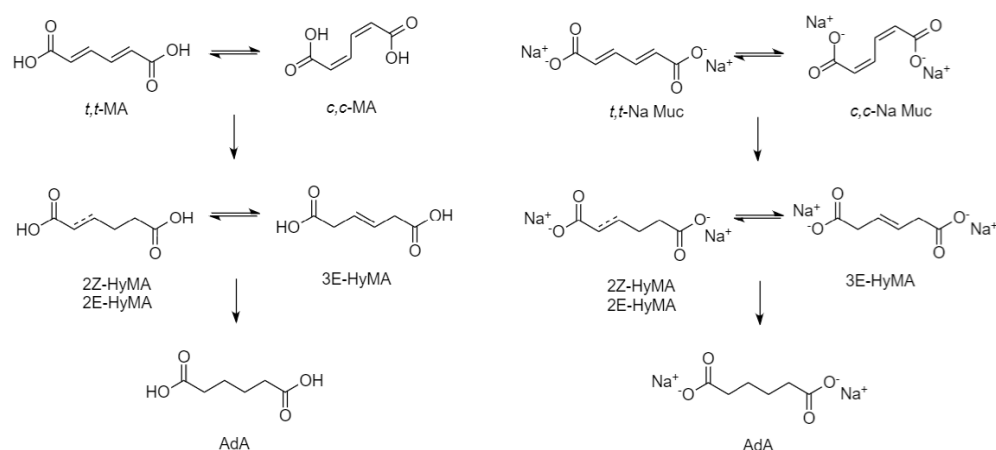


Figure 1. Reaction scheme for AdA production starting from different substrates: MA (left) and Na-Muc (right).

On the catalyst with the highest activity, 1%Pd/HHT-P, the influence of metal/substrate ratio and temperature was investigated. All the catalysts used in the reactions were characterized by inductively coupled plasma optical emission spectroscopy (ICP-OES), X-ray Photoelectron Spectroscopy (XPS) and Scanning Transmission Electron Microscopy (STEM) analysis. The full characterization of the fresh catalysts can be found in the paper of Barlocco et al. [31].

In summary, this work aims to address the environmental challenges associated with traditional nylon production by developing more sustainable catalytic processes for producing bio-adipic acid. By employing innovative functionalized carbon supports and exploring both CDH and CTH processes, the aim is to demonstrate improved catalytic performance, stability, and selectivity, contributing to greener and more efficient industrial processes. This innovative approach not only highlights the advantages of this materials over those in the literature but also underscores the potential for significant environmental benefits. Specifically, the use of CTH with formic acid as a hydrogen donor represents a significant innovation, offering a safer, more cost-effective, and environmentally friendly alternative to traditional hydrogenation methods.

2. Results

Two different supports were synthesized starting from bare high-temperature heat-treated carbon nanofibers (HHT-CNFs) and functionalizing them with HNO₃ and H₃PO₄

to obtain HHT-O and HHT-P. Using these supports, palladium-based catalysts with a metal loading of 1% were synthesized and the following catalysts were obtained: 1%Pd/HHT, 1%Pd/HHT-O and 1%Pd/HHT-P. Sol immobilization technique was chosen, since it allows an homogeneous distribution of the small NPs on the support, working at room temperature and with low production costs [30].

These catalysts were previously characterized and tested in FAD with good results, particularly for the catalysts synthesized using the functionalized supports that show an enhance of the catalytic activity and stability in respect of that obtained with bare HHT [31].

Since these results, it was decided to test them in the CTH process using the FA as hydrogen donor to hydrogenate the MA forming AdA. The first step was to investigate the behaviour of these three catalysts in the catalytic direct hydrogenation of MA using molecular hydrogen gas.

2.1. Catalytic Direct Hydrogenation of MA

The three catalysts were tested at the same conditions in catalytic direct hydrogenation of muconic acid: reactions were carried out at 70 °C, at 3 bar absolutes of hydrogen with a catalysts/substrate molar ratio of 1/500. To have a first understanding of their behaviour the initial activity, the conversion of muconic acid and the yield of adipic acid were evaluated using Equation (5), Equation (3) and Equation (4), respectively. As it possible to observe in Figure 2, all the catalysts have a good initial activity, comparable with those obtained in other previous study [32], but the functionalized ones show better results, namely 2362.5 h⁻¹ and 1805.5 h⁻¹ for 1% Pd/HHT-O and 1% Pd/HHT-P respectively, compared to 1200.0 h⁻¹ for 1% Pd/HHT. Among all, the Pd/HHT-O shows the highest initial activity, 97% higher than Pd/HHT and 31% than Pd/HHT-P; while Pd/HHT-P has an initial activity 50% higher than Pd/HHT. Also in the case of FAD [31], the oxygenated catalyst had shown the highest value of initial activity in respect to the others.

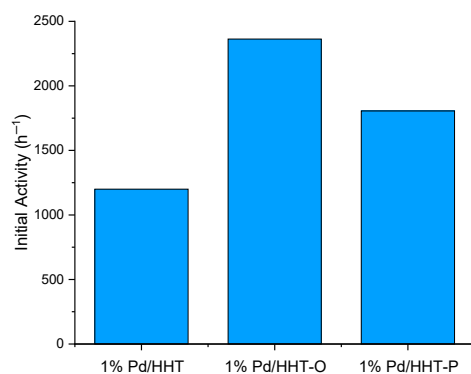


Figure 2. Initial activity (h⁻¹) of the three different catalysts for the CDH process calculated after 5 min of reaction using the Equation (5).

In Figure 3, the reaction courses for the three different catalysts are depicted. Kinetic profiles for the three catalysts were examined after 2 h of reaction (Figure 3). A similar reaction profile was obtained for both functionalised catalysts, showing a higher conversion in respect to the Pd/HHT. In addition to the conversion of muconic acid and the production of adipic acid, the formation trend of intermediates can also be observed. These intermediates reach their peak concentration at 15 min and then rapidly decrease, leading to the formation of adipic acid. This phenomenon is more pronounced with the catalysts that have functionalized supports, suggesting greater efficiency in the conversion of muconic acid to adipic acid. Nevertheless, the two functionalized catalysts do not achieve complete conversion to adipic acid, instead reaching a plateau at around 80%. This plateau is due to the persistence of intermediates, particularly the 3E-HyMA (Figure 1), which is hardly converted to adipic.

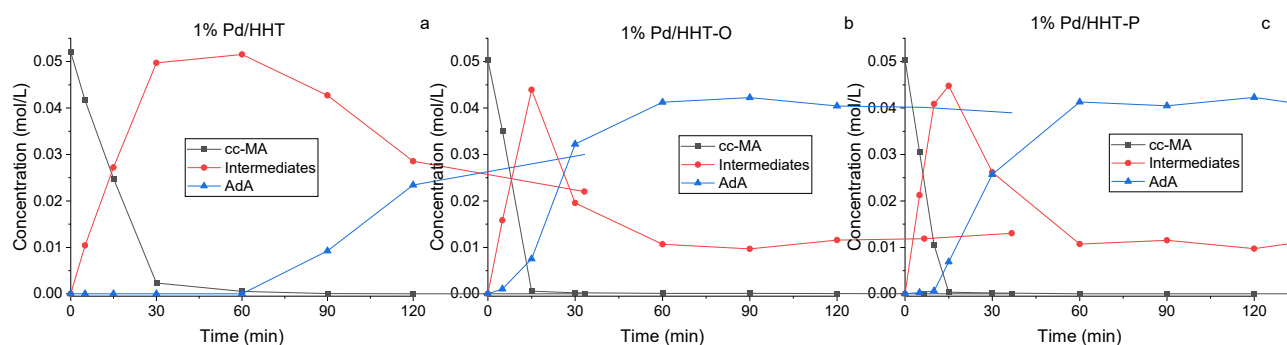


Figure 3. Comparison of the reaction courses for the three different catalysts in the catalytic direct hydrogenation: (a) 1%Pd@HHT, (b) 1%Pd@HHT-O, (c) 1%Pd@HHT-P. Reaction conditions: MA concentration 0.05 M, temperature 70 °C, 3 bar pressure of H₂, metal/substrate molar ratio 1/500, 1200 rpm.

More in detail, after an hour all the three catalysts lead to complete conversion of muconic acid, therefore more interesting is the comparison at 5 and 15 min of reaction. The functionalized HHT catalyst (Pd/HHT-O, Pd/HHT-P), reach complete conversion already after 15 min, maintain a higher rate of consumption of muconic acid also after the starting phase of the reaction (Table 1).

Table 1. Summary of the catalytic results in the catalytic direct hydrogenation of MA. Reaction conditions: MA concentration 0.05 M, temperature 70 °C, 3 bar pressure of H₂, metal/substrate molar ratio 1/500, 1200 rpm.

Catalysts	MA Conversion after 5 min (%)	MA Conversion after 15 min (%)	MA Conversion after 60 min (%)
1%Pd/HHT	20	52	100
1%Pd/HHT-O	39	100	100
1%Pd/HHT-P	31	100	100

From previous studies [33] it is known that production of adipic acid occurs in a two-step reaction through the formation of reaction intermediates (Figure 1), where to reach the last product a quite complete conversion of muconic acid is required.

As a proof of this, it is possible to observe how in the case of the non-functionalized HHT catalyst (Pd/HHT), where the complete conversion of muconic acid was reached after 60 min, there isn't formation of adipic acid before the first hour of reaction. While in the case of Pd/HHT-O and Pd/HHT-P, there is already production of adipic acid after 15 min of reaction (Figures 3 and 4).

Functionalized catalysts (Pd/HHT-O, Pd/HHT-P) not only give a better and faster conversion, but also a higher yield of adipic acid, reaching respectively 80% and 84% yield of AdA after two hours, with a quite similar profile. Regarding Pd/HHT, it has a different trend with a slower formation of adipic acid and a yield of just 58% after two hours.

The increased catalytic performance of the functionalized catalysts can be explained by comparing the dimension of Pd NPs detected by TEM analysis. The functionalization allowed to obtain smaller NPs, with an average particle size that decrease from 3 nm to 2.3 nm when the treated supports are used.

In addition, the XPS analysis revealed an increase in the Pd exposure after O and P functionalization Pd/HHT-P (1.57%) > Pd/HHT-O (1.14%) > Pd/HHT (0.77%) as we will detail below. This rise is indicative of a higher concentration of active sites.

Comparing the results obtained in this work with others found in literature, it is possible to state that the novel catalysts lead to comparable or better results, reaching full conversion and high AdA yield, working both at low temperature and pressure but also using a low quantity of catalyst (Table 2).

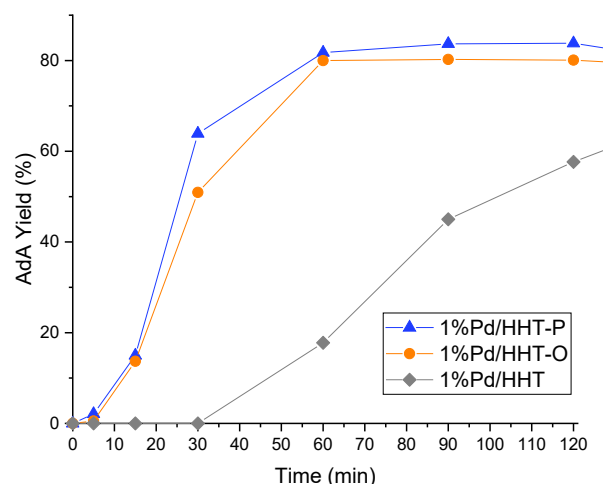


Figure 4. AdA Yield monitored along time in the catalytic direct hydrogenation of MA. Reaction conditions: MA concentration 0.05 M, temperature 70 °C, 3 bar pressure of H₂, metal/substrate molar ratio 1/500, 1200 rpm.

Table 2. Published results about MA and Na-Muc hydrogenation reactions performed using water as solvent.

Catalysts	Substrate	T [°C]	H ₂ [bar]	MA Conv (Time) [%]	AdA Yield [%]	Metal/Substrate Ratio [mol/mol]	Ref.
10%Pt/AC	MA	25	3.5	100 (3 h)	90	1/4	[4]
10%Pt/AC	MA	25	34	100 (2.5 h)	97	1/20	[34]
5%Pt/AC	Na-Muc	70	4	100 (2 h)	100	1/275	[35]
5%Pd/AC	MA	70	1	100 (60 min)	100	1/200	[36]
5%Pd/AC	Na-Muc	70	1	100 (90 min)	95	1/200	[36]
1% Pd/KB	Na-Muc	50	1	100 (90 min)	53	1/200	[37]
1%Pd/Norit	Na-Muc	50	1	100 (90 min)	20	1/200	[37]
1%Pd/G60	Na-Muc	50	1	100 (90 min)	27	1/200	[37]
1%Pd ₈ Au ₂ /HHT	MA	50	2	100 (200 min)	90	1/1500	[32]
1%Pd ₈ Zn ₂ /HHT	Na-Muc	70	2	100 (180 min)	84	1/500	[38]
1%Pd ₈ Ni ₂ /HHT	Na-Muc	70	2	100 (180 min)	80	1/500	[38]
1%Pd/HHT	Na-Muc	70	3	100 (120 min)	58	1/500	
1%Pd/HHT-O	Na-Muc	70	3	100 (120 min)	80	1/500	Current work
1%Pd/HHT-P	Na-Muc	70	3	100 (120 min)	84	1/500	

What is most affected by the functionality of the support is the stability of the catalyst. In fact, most heteroatoms enhance the electron density of the neighbouring carbon atoms increasing the back-donation from C to the metal atoms, leading to a stronger binding between the support and the NPs and preventing sintering problems [39,40]. Therefore, to evaluate the stability of the three catalysts, recycle tests were conducted. For this, 6 consecutive runs of 2 h each were performed and after every run the catalyst was recovered by filtration, washed and reused.

As expected, Pd/HHT underwent degradation from the third run onwards (Figure 5). Differently, the functionalized catalysts maintained a MA conversion above 90% for up to six consecutive reactions and in particular in the case of 100% till the fourth recycle (Figure 5a). Even in the case of adipic acid production, only the two functionalized catalysts continued to produce AdA up to the sixth run (Figure 5b).

The Pd/HHT-P confirms to be the catalyst with greater stability among the three, showing in any case a constant decrease in the yield of AdA. Therefore, even in this case, the presence of a functionalized support allowed for the synthesis of a more stable and active catalyst.

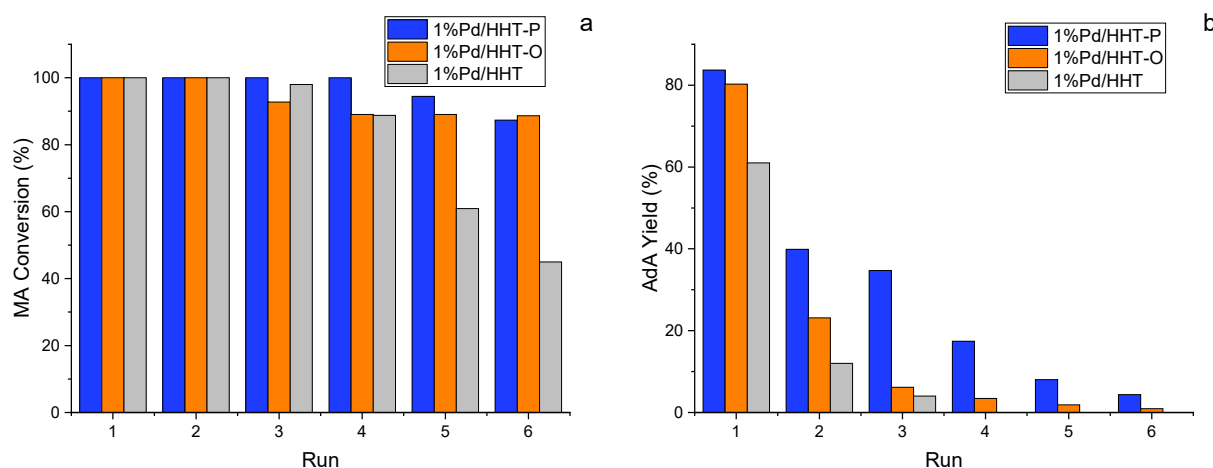


Figure 5. (a) MA conversion and (b) Yield of AdA after 120 min during recycling tests in the catalytic direct hydrogenation of MA. Reaction conditions: MA concentration 0.05 M, temperature 70 °C, 3 bar pressure of H₂, metal/substrate molar ratio 1/500, 1200 rpm.

To deepen if the deactivation was caused by the metal leaching, inductively coupled plasma optical emission spectroscopy (ICP-OES) analyses were performed. In the case of the two functionalized catalysts only a slight loss of palladium was detected (0.1% for Pd/HHT-O and 0.12% for Pd/HHT-P). On the contrary, the amount of Pd supported on the bare HHT decreases from 1% to 0.78% after the reaction, confirming the leaching of the metal.

The higher stability obtained with the functionalized catalysts can be explained by the DFT investigation presented in the work of Barlocco et al. [31], where an array of fifteen Pd atoms on various carbon substrates was studied. The adhesion energies (E_{ADH}) between the surface and the cluster on all functionalized surfaces were higher than those of the Pd supported on the bare surface, indicating that the functionalization increased the stability of the Pd atoms. The following are the reported values obtained: Pd/G_COOH –3.028 eV, Pd/G_OH –3.023 eV, Pd/G_CO –3.678 eV, and Pd/G_PO3H –2.494 eV.

These results confirm the stabilization of the metal NPs deriving from the addition of heteroatoms to the carbon structures [28].

2.2. Catalytic Transfer Hydrogenation

Since the good catalytic activity and stability obtained in the CDH process, the three catalysts were also tested in the catalytic transfer hydrogenation of MA using FA as hydrogen donor.

For these tests, it was decided to start working with sodium muconate as in the case of the CDH process. However, the reaction does not lead to conversion of muconic except in low percentage (between 10 and 20%). The observed behaviour can likely be attributed to the salification of formic acid (FA) during the addition of sodium hydroxide (NaOH) to the solution. This salification process may have interfered with the release of hydrogen from the hydrogen donor, consequently affecting the overall reaction dynamics. Thereafter, three experimental tests were conducted using ccMA. Also in this case, a large excess of FA was used and working with these conditions it was possible to obtain substrate conversion and, in some cases, the production of adipic.

In Figure 6, the reaction courses for the three different catalysts are depicted. With the catalyst supported on bare HHT, no production of AdA was observed throughout the reaction time (Figure 6a). Additionally, the conversion of MA was low, reaching a maximum of 35% after 240 min. Conversely, for both catalysts supported on functionalized carbon nanofibers, a higher catalytic activity was evident. In the case of Pd/HHT-O (Figure 6b), although no AdA production was detected during the initial reaction period, there was an improvement in catalytic activity compared to Pd/HHT, achieving a 61%

conversion of MA after 240 min and an increase in the production of intermediates over time. Consequently, the reaction was extended to 360 min, where a stabilization in the production of intermediates was observed, leading to the initiation of AdA production, with a yield of 19% at the conclusion of the reaction. Indeed, given the kinetics of the process through a two-step hydrogenation process, the first hydrogenation reaction is the fastest reaction step, while to completely hydrogenate the intermediates, more energy is required. This explains the measured longer persistency of the intermediate during the reaction courses [33]. In Figure 6c the reaction course of the last tested catalyst is presented. In this case a rapid first hydrogenation step can be observed, with a conversion of 24% and 75% after 15 and 60 min respectively, and a total conversion already at two hours. In addition, a typical pattern of this reaction can be observed with regard to the concentration of the intermediates. It is therefore possible to say that the Pd/HHT-P catalyst has a reaction pattern similar to that shown in the CDH, with good catalytic properties even in the formic acid mediated process.

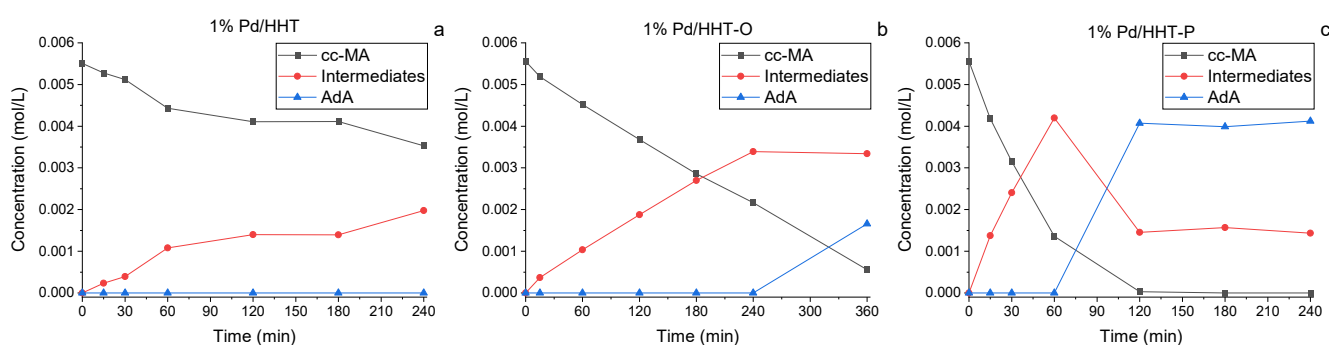


Figure 6. Comparison of the reaction courses for the three different catalysts in the catalytic transfer hydrogenation: (a) 1%Pd@HHT, (b) 1%Pd@HHT-O, (c) 1%Pd@HHT-P. Reaction conditions: MA concentration 0.005 M, metal/substrate molar ratio 1/65, temperature 70 °C, pressure of N₂ 3 bar, MA/FA ratio 1/10, 1200 rpm.

Since the metal/substrate ratio used for the CTH reaction is elevated, the next was to try to decrease this value. For this study, the catalyst that previously showed increased catalytic activity, namely 1%Pd/HHT-P, was examined. Three different ratios were investigated, namely 1/65, 1/100 and 1/125. Both MA conversion (Figure 7a) and AdA yield (Figure 7b) decrease with the lowering of the metal/substrate ratio, as expected. Despite the evident decrease in the catalytic performance, the 1/100 ratio still shows an AdA yield of 30% after 4 h of reaction.

To try to raise this yield, another important parameter was investigated maintaining 1/100 as metal/substrate ratio, namely the temperature. Three different values were taken into consideration, namely 50 °C, 70 °C and 90 °C. MA conversion (Figure 8a) and AdA yield (Figure 8b) were evaluated along the time, finding that the conversion of the substrate increased linearly as the temperature rose. The same held true for adipic yield, which achieved 80% after 3 h working at 90 °C. This result was very promising and encouraging for other study. Indeed, it indicates that optimizing the reaction parameters it is possible to achieve satisfactory yield of adipic acid utilizing formic acid instead of pure hydrogen gas.

These results were compared with those obtained in a previous work [26] (Table 3), where bimetallic palladium catalysts were used in FAD and CTH processes. The addition of rhodium as second metal led to an enhancement of the catalytic activity and the stability in respect to the monometallic catalyst. All the tested catalysts showed good activity for the first step of the reaction, however only using bimetallic catalysts the formation of adipic acid was enhanced. On the contrary, with the present work, it was found that also monometallic palladium, thanks to the functionalization of the support, can lead to the formation of bio-adipic acid. Furthermore, optimizing the working conditions, a higher AdA yield in respect to the previous obtained was reached.

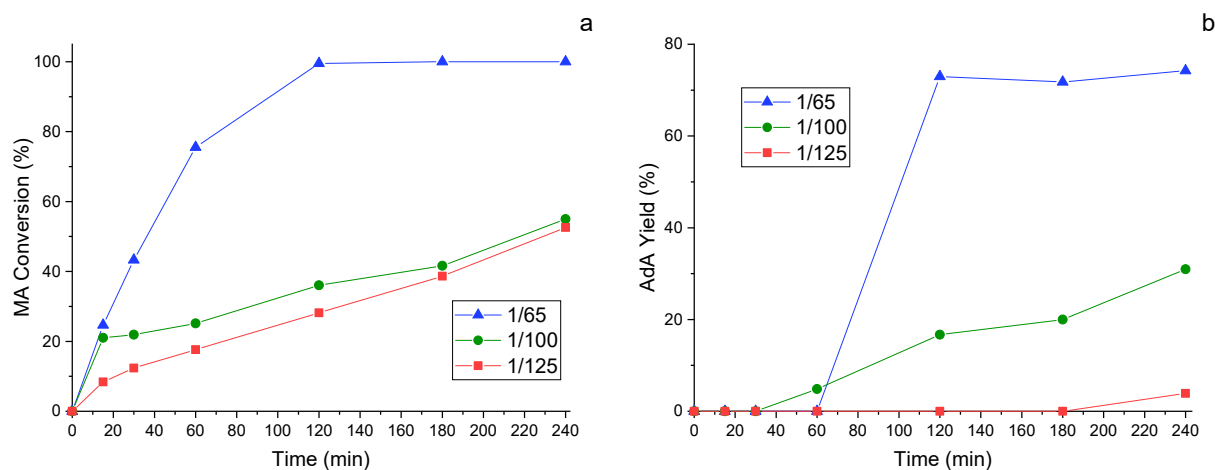


Figure 7. Study of the influence of the metal/substrate ratio: 1/65, 1/100 and 1/125 in the catalytic transfer hydrogenation: (a) MA conversion and (b) AdA Yield monitored along time. Reaction conditions: MA concentration 0.005 M, temperature 70 °C, pressure of N₂ 3 bar, MA/FA ratio 1/10, 1200 rpm.

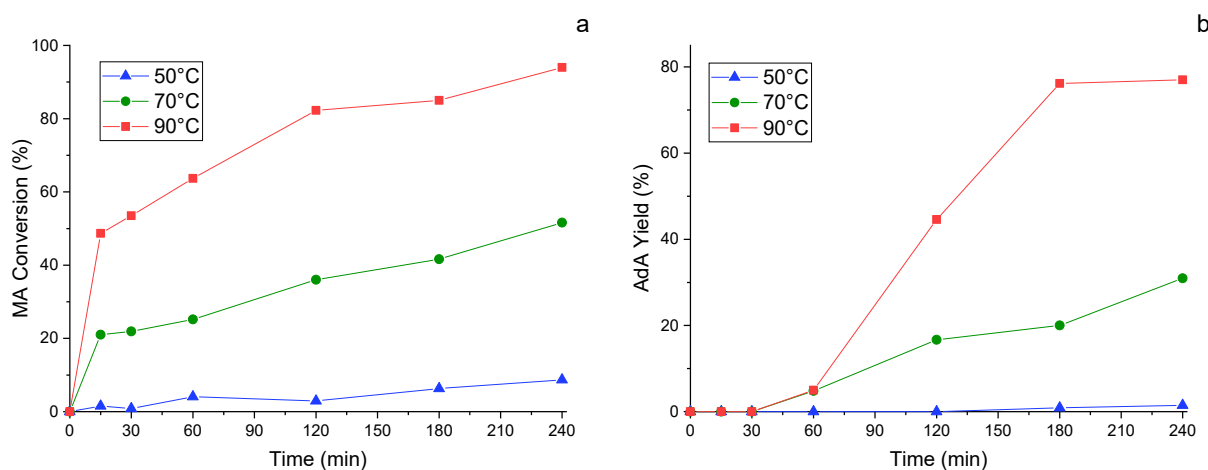


Figure 8. Study of the influence of the temperature. (a) MA conversion and (b) AdA Yield monitored along time. Reaction conditions: MA concentration 0.005 M, metal substrate molar ratio 1/100, pressure of N₂ 3 bar, MA/FA ratio 1/10, 1200 rpm.

Table 3. Results about CTH process using MA as substrate and FA as hydrogen donor.

Catalysts	MA/FA Ratio [mol/mol]	T [°C]	N ₂ [bar]	MA Conv (Time) [%]	AdA Yield [%]	Metal/Substrate Ratio [mol/mol]	Ref.
1%Pd/HHT	1/4	30	-	85 (6 h)	0	1/200	[26]
1%Pd ₉₀ Rh ₁₀ /HHT	1/4	30	-	85 (6 h)	21	1/200	
1%Pd ₆₉ Rh ₃₁ /HHT	1/4	30	-	85 (6 h)	36	1/200	
1%Pd/HHT	1/10	70	3	40 (4 h)	0	1/65	Current work
1%Pd/HHT-O	1/10	70	3	89 (6 h)	18	1/65	
1%Pd/HHT-P	1/10	70	3	100 (4 h)	74	1/65	
1%Pd/HHT-P	1/10	90	3	94 (4 h)	77	1/100	

2.3. Characterization

The materials used in this work were previously fully characterized in the paper of Barlocco et al. [31]. Briefly, XPS analyses were employed to investigate the surface of the catalysts employed here. The final Pd based materials showed an increased metal exposure after P and O functionalisation (Table 4). Moreover, it was observed that palladium

preferentially deposited on P and O functionalities, because P content on 1 wt%Pd@P-HHT and O content on 1 wt%Pd@O-HHT decreased after Pd deposition and P and O leaching was not observed.

Table 4. XPS results from O, P and Pd high resolution (HR) spectra.

Sample	Atomic Ratio (%) C-O-P-Pd	B.E. (eV) % At.	O 1s			P 1s	Pd 3d	
			C=O, P=O, P-O	C-O, C-O-C, P-O-C	COOH	C-O-PO ₃ , C-P	Pd ²⁺	Pd ⁰
HHT	99.1-0.9-0.0-0.0	B.E. (eV) % At.	531.2 50.4	533.0 48.4	534.1 1.2	- -	- -	- -
HHT-O	92.2-77.8-0.0-0.0	B.E. (eV) % At.	531.3 54.8	532.9 35.3	533.9 8.5	- -	- -	- -
HHT-P	93.5-4.8-1.4-0.0	B.E. (eV) % At.	531.4 61.3	533.0 33.2	534.2 5.5	134.2 100	- -	- -
Pd/HHT	96.5-2.7-0.0-0.8	B.E. (eV) % At.	531.3 49.8	533.2 49.2	534.3 1.0	- -	336.4 38.5	335.0 61.5
Pd/HHT-O	92.1-6.5-0.0-1.1	B.E. (eV) % At.	531.2 56.3	533.2 33.4	534.2 10.7	- -	336.8 43.5	335.0 56.5
Pd/HHT-P	93.1-4.7-0.6-1.6	B.E. (eV) % At.	531.4 58.5	532.8 27.0	534.4 14.5	133.9 100	336.5 22.9	334.8 77.1

The composition of the catalysts was also analysed by STEM-EDS mapping. Figure 9 shows some relevant HR-STEM images of the samples. It could be observed that Pd nanoparticles are, in general, homogeneously distributed on the carbon nanotube surface, although some agglomerations are observed. The average particle size decreases from 3 nm to 2.3 nm when the treated supports are used. For the 1 wt%Pd@HHT catalyst, a nearly unimodal distribution centered around 3 nm was detected. In contrast, when palladium is supported on the two functionalized carbons, a bimodal particle size distribution was observed due to a significant increase in the number of particles smaller than 2 nm. This increase in smaller particles leads to an enhancement in the dispersion of Pd nanoparticles, raising it from 36% to 42% and confirming that the functionalization treatments allow to improve the dispersion of metal NPs. The composition of the sample was analysed by STEM-EDS mappings. Also, in this case some Pd NPs are in contact with phosphorous, confirming what it was previously observed in the XPS spectra.

CHN elemental analysis was performed to confirm that the non-functionalized catalyst presents the higher percentage of C on the total weight, obtaining a value of 98.3% in respect to 97.7% and 95.6% for Pd/HHT-P and Pd/HHT-O respectively. In addition, the Pd/HHT-P catalyst present a percentage of H of 1.1%, whose value is higher than the other two catalysts; in fact, they present a value of 0.7 % and 0.7% respectively for Pd/HHT and Pd/HHT-O. Moreover, the latter present 0.07% of N, element that is not revealed in the other catalysts. This can be explained due to the higher quantity of HNO₃ used for the functionalization.

Finally, TGA analysis were performed in order to check the stability of the materials at high temperature in the range 30–120 °C, i.e., beyond the conditions of use in our experimental tests. The results confirmed the stability of all the catalysts in this temperature interval.

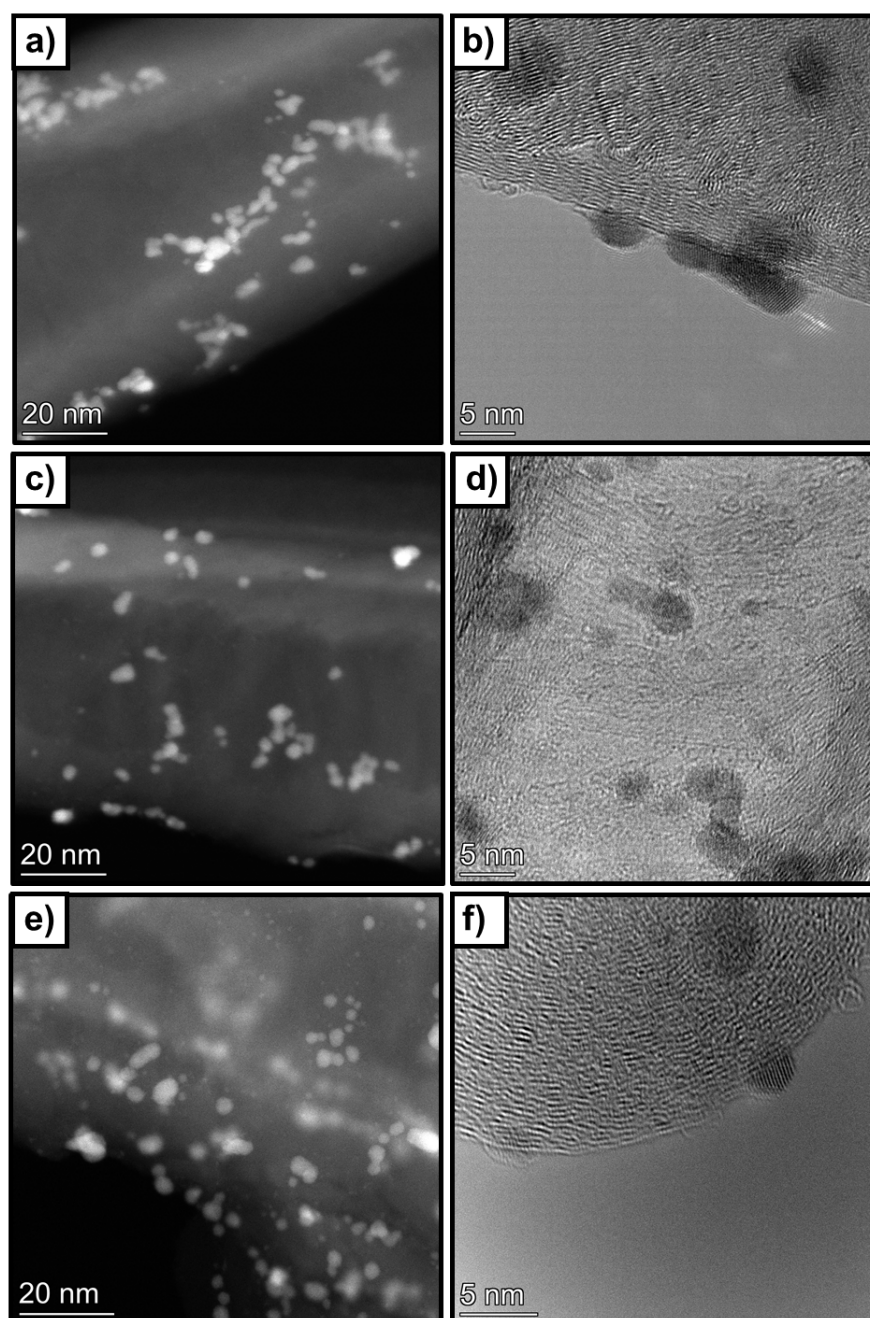


Figure 9. Representative HR-STEM images of. (a,b) 1wt%Pd@HHT, (c,d) 1wt%Pd@P-HHT and (e,f) 1wt%Pd@O-HHT.

3. Materials and Methods

3.1. Materials and Chemicals

Sodium tetrachloropalladate (II) (Na_2PdCl_4 , 99.99%), sodium borohydride (NaBH_4 , 99.99%) and polyvinyl alcohol (PVA, average molar weight 10,000, 87–89% hydrolysed) were purchased from Merck (Haverhill, MA, USA) and used without any pre-treatment. All the catalytic tests were carried out using *cis,cis*-muconic acid (Merck, $\geq 97\%$) and formic acid ($\geq 95\%$, Sigma-Aldrich, St. Louis, MO, USA) as substrates and deionised water ($\geq 99\%$, Sigma-Aldrich, St. Louis, MO, USA) as the solvent. CNFs PR24- HHT (High Heat-Treated carbon nanofiber), used as support, were obtained from Applied Science Company (Cedarville, OH, USA).

3.2. Catalyst Synthesis

All the catalysts were previously synthesised [31] by a typical sol immobilisation procedure [30], using PVA as capping agent (M/PVA = 1/0.5 (wt/wt)) and NaBH₄ as reducing agent (M/NaBH₄ = 1/8 mol/mol). The metal loading for each catalyst was 1% wt of Pd. In this way three different catalysts were synthesized, namely 1%Pd/HHT, 1%Pd/HHT-O and 1%Pd/HHT-P.

For the support functionalization the bare High Heat-Treated Carbon Nanofiber (HHT-CNFs) were functionalized using a mixture 1:1 vol/vol of HNO₃ (65% wt) and H₃PO₄ (≥99% wt) and pure HNO₃ (65% wt) to obtain respectively HHT-P and HHT-O.

3.3. Catalytic Tests

3.3.1. Catalytic Direct Hydrogenation

The catalytic direct hydrogenation of MA using molecular hydrogen has been carried out using the sodium muconate (Na-Muc) salt to get as close as possible to the post-fermentation conditions of the biomass [6]. In addition, using the sodium muconate salt allows for a substrate concentration higher than 1.42×10^{-2} M, which is not feasible for example with trans,trans-muconic acid (t,t-MA) due to its solubility limitations [36] in water.

The hydrogenation of muconic acid to bio-adipic acid was carried out in a 100 mL autoclave equipped with a magnetic stirrer, a thermocouple, and a pressure controller. The reactions were carried out at 70 °C and the reactor was pressurized at 3 bar absolute of hydrogen. The reactions were performed with a catalysts/substrate ratio of 1/500 and at 1200 rpm, allowing to keep a kinetic regime and to avoid diffusional limitations. Typically, 25 mL of a 0.05 M demineralized water solution of Na-Muc were prepared by adding 178 mg (1.25 mmol) of cis,cis-muconic acid (cc-MA) and 2 equivalent (2.5 mmol) of NaOH and then sonicating the resulting suspension until the solid was completely dissolved.

The reaction was carried out for 3 h monitored by sampling after 5, 10, 15, 30 min for the first part of the reaction and then every 30 min till the end of the reaction. The reaction samples were quenched in the vials and the catalyst was removed. The reaction products were analysed using high-performance liquid chromatography (HPLC) with an ultraviolet (UV) detector set at 210 nm and a Rezex ROA-Organic Acid H+ (8%) column. This setup enabled the separation of all intermediates, substrates, and adipic acid (AdA) to assess muconic acid (MA) conversion and product selectivity [32].

Recycle tests were carried out with the same setup used for the hydrogenation reaction. Every reaction was conducted for 120 min. After this time, the catalyst was then filtered, washed with deionized water, and reused for the next run. With this procedure, it was possible to evaluate MA conversion for 6 consecutive cycles. The remaining aqueous residue from filtration was separately collected and analysed by inductively coupled plasma (ICP) to evaluate palladium leaching into the solution during the reactions.

The MA conversion was evaluated using Equation (3)

$$\text{Conversion}(\%) = \frac{\text{mol}_{\text{IN}} - \text{mol}_{\text{OUT}}}{\text{mol}_{\text{IN}}} \cdot 100 \quad (3)$$

where mol_{IN} are the moles of the substrate initially used for the reaction while mol_{OUT} are the moles of the substrate that remain after the reaction.

Products yield of AdA was evaluated using Equation (4).

$$\text{Yield}_n(\%) = \frac{\text{mol}_n}{\text{mol}_n + \sum \text{mol}_i} \cdot \text{Conversion}(\%) \quad (4)$$

where mol_n is the number of moles of the considered reaction product, in this case AdA, Σmol_i is the sum of the moles of all the products and conversion is calculated using Equation (3).

Initial activity after 5 min of reaction was evaluated using the Equation (5) and considering the MA reacted moles (after 5 min) and the total metal amount used for the reaction.

$$\text{Initial activity} \left(\text{h}^{-1} \right) = \frac{\text{mol}_{\text{MAreacted}}}{\text{mol}_{\text{Pd}} \cdot \text{reaction time (h)}} \quad (5)$$

3.3.2. Catalytic Transfer Hydrogenation

In the case of catalytic transfer hydrogenation of MA using FA as hydrogen donor, the reaction has been carried out starting both from Na-Muc salt and cc-MA as substrates. The reaction proceeds in the same way and with the same intermediates (Figure 1).

The reaction was carried out with the same apparatus of the CDH. In this case all the reactions were conducted in nitrogen atmosphere. The reactions were carried out at 70 °C and the reactor was pressurized at 3 bar absolutes of nitrogen. The reactions were performed with a catalysts/substrate ratio of 1/65 and at 1200 rpm. Typically, 25 mL of a 0.005 M demineralized water solution of cis,cis-muconic acid was prepared by adding 18 mg (0.125 mmol) of cc-MA, and then sonicating until complete dissolution. In the case of Na-Muc as substrate, and 2 equivalent (0.25 mmol) of NaOH was added at the solution. After that, 50 µL of formic acid (MA/FA = 1/10 (mol/mol)) was added. Then the solution was placed in the reactor and the reaction was started.

The reaction was monitored by sampling after 15, 30, 60, 90, 120, 180 and 240 min, after quenching the reaction in the sample vials. The reaction products were analysed with HPLC using the same method presented before.

On the catalyst that had shown the best catalytic behaviour, namely 1%Pd/HHT-P, the influence of metal/substrate ratio (1/65, 1/100, 1/125) and temperature (50, 70 and 90 °C) was investigated.

3.4. Catalyst Characterisation

The materials used in this work were previously fully characterized in the paper of Barlocco et al. [31].

Samples were characterized by X-ray photoelectron spectroscopy (XPS). Thermo Scientific K-alpha+ spectrometer (Thermo Fisher Scientific, Waltham, MA, USA) was used for XPS measurements. The samples were analysed using a monochromatic Al X-ray source operating at 72 W, with the signal averaged over an oval-shape area of 600 × 400 µ. Data were recorded at 150 eV for survey scans and 40 eV for high resolution (HR) scans with a 1 eV and 0.1 eV step size, respectively. CASAXPS (v2.3.17 PR1.1) was used for the analysis of the data, using Scofield sensitivity factors and energy exponent of −0.6.

Transmission electron microscopy characterisation was carried out on a double Cs aberration-corrected FEI Titan [41] Themis 60–300 microscope equipped with a monochromator, a X-FEG gun and a high efficiency XEDS ChemiSTEM, which consists of a 4-windowless SDD detectors. HR-STEM images were recorded at 200 kV and using a high-angle annular dark-field (HAADF) detector with a camera length of 11.5 cm.

CHN elemental analysis was carried out on PerkinElmer precisely Series II CHNS analyser.

Thermogravimetric analysis (TGA) was performed using a TGA 2 Star system provided by Mettler Toledo. Measurements were performed using a heating ramp of 10 °C/min between 30 °C and 800 °C in a constant flow of nitrogen and values were collected every second.

Metal loading and metal leaching were analysed by inductively coupled plasma optical emission spectroscopy (ICP-OES) using a Perkin Elmer Optima 8000 emission (PerkinElmer, Waltham, MA, USA).

4. Conclusions

Muconic acid hydrogenation to bio-adipic acid was investigated using palladium-based catalysts. The metal NPs were supported on high-temperature heat-treated carbon

nanofibers (HHT-CNFs) and to assess the impact of support functionalization on catalyst stability, the HHT-CNFs were further functionalized with phosphorus and oxygen to obtain HHT-P and HHT-O, respectively. These catalysts were tested in the production of AdA via two distinct methodologies: catalytic direct hydrogenation of muconic acid using molecular hydrogen and catalytic transfer hydrogenation utilizing formic acid as hydrogen donor. The results are characterized by an enhancement of the catalytic performance for the functionalized catalysts for both the process. In the CDH reaction an AdA yield of about 80% for both the catalysts was reached in contrast with 60% of Pd/HHT. In the case of the CTH process, only the catalyst containing 1 wt% Pd supported on HHT-P exhibited satisfactory results, reaching a MA conversion of 100% and an AdA yield of 74%. In addition, an increase of the stability has been obtained for the functionalized catalysts in respect of that supported on bare HHT, confirm the stabilization of the metal NPs deriving from the addition of heteroatoms to the carbon structures.

Further studies should focus on the optimization of the reaction conditions for the CTH process, including temperature, pressure, and catalyst concentration, in order to obtain comparable results with the CDH ones and to ensure the effective management of intermediate concentrations and the successful transition to the final hydrogenation stage that led to the production of adipic acid.

Author Contributions: Conceptualization, E.Z. and C.P.; methodology, E.Z. and C.P.; software, E.Z., S.F. and I.B.; validation, E.Z., S.F. and C.P.; formal analysis, E.Z., S.F., M.S. and C.P.; investigation, E.Z., S.F. and N.J.; resources, C.P.; data curation, E.Z., S.F. and I.B.; writing—original draft preparation, E.Z., S.F. and I.B.; writing—review and editing, all of the authors; visualization, all of the authors; supervision, E.Z. and C.P.; project administration, C.P.; funding acquisition, C.P. All authors have read and agreed to the published version of the manuscript.

Funding: This research received no external funding.

Data Availability Statement: Please write to elisa.zanella@unimi.it for the research data availability.

Conflicts of Interest: The authors declare no conflicts of interest.

References

1. Thiemens, M.H.; Trogler, W.C. Nylon Production: An Unknown Source of Atmospheric Nitrous Oxide. *Science* **1991**, *251*, 932–934. [[CrossRef](#)] [[PubMed](#)]
2. Tonsi, G.; Maesani, C.; Alini, S.; Ortenzi, M.A.; Pirola, C. Nylon Recycling Processes: A Brief Overview. *Chem. Eng. Trans.* **2023**, *100*, 727–732. [[CrossRef](#)]
3. Kruyer, N.S.; Peralta-Yahya, P. Metabolic Engineering Strategies to Bio-Adipic Acid Production. *Curr. Opin. Biotechnol.* **2017**, *45*, 136–143. [[CrossRef](#)] [[PubMed](#)]
4. Draths, K.M.; Frost, J.W. Environmentally Compatible Synthesis of Adipic Acid from D-Glucose. *J. Am. Chem. Soc.* **1994**, *116*, 399–400. [[CrossRef](#)]
5. Almqvist, H.; Veras, H.; Li, K.; Garcia Hidalgo, J.; Hulteberg, C.; Gorwa-Grauslund, M.; Skorupa Parachin, N.; Carlquist, M. Muconic Acid Production Using Engineered *Pseudomonas Putida* KT2440 and a Guaiacol-Rich Fraction Derived from Kraft Lignin. *ACS Sustain. Chem. Eng.* **2021**, *9*, 8097–8106. [[CrossRef](#)]
6. Johnson, C.W.; Salvachúa, D.; Khanna, P.; Smith, H.; Peterson, D.J.; Beckham, G.T. Enhancing Muconic Acid Production from Glucose and Lignin-Derived Aromatic Compounds via Increased Protocatechuate Decarboxylase Activity. *Metab. Eng. Commun.* **2016**, *3*, 111–119. [[CrossRef](#)] [[PubMed](#)]
7. Bäckvall, J.-E. Transition Metal Hydrides as Active Intermediates in Hydrogen Transfer Reactions. *J. Organomet. Chem.* **2002**, *652*, 105–111. [[CrossRef](#)]
8. Lakshminarayana, B.; Satyanarayana, G.; Subrahmanyam, C. Bimetallic Pd–Au/TiO₂ Nanoparticles: An Efficient and Sustainable Heterogeneous Catalyst for Rapid Catalytic Hydrogen Transfer Reduction of Nitroarenes. *ACS Omega* **2018**, *3*, 13065–13072. [[CrossRef](#)] [[PubMed](#)]
9. Baráth, E. Hydrogen Transfer Reactions of Carbonyls, Alkynes, and Alkenes with Noble Metals in the Presence of Alcohols/Ethers and Amines as Hydrogen Donors. *Catalysts* **2018**, *8*, 671. [[CrossRef](#)]
10. Samec, J.S.M.; Bäckvall, J.-E.; Andersson, P.G.; Brandt, P. Mechanistic Aspects of Transition Metal-Catalyzed Hydrogen Transfer Reactions. *Chem. Soc. Rev.* **2006**, *35*, 237–248. [[CrossRef](#)]
11. Letelier, K.; Parra-Melipan, S.; Negrete-Vergara, C.; López, V.; Valdebenito, G.; Artigas, V.; Aranda, B.; Vega, A.; Moya, S.A.; Aguirre, P. High Activities of Nickel (II) Complexes Containing Phosphorus-Nitrogen Ligands in Hydrogen Transfer Reaction of Imines Using Formic Acid as a Renewable Hydrogen Source. *Mol. Catal.* **2023**, *546*, 113262. [[CrossRef](#)]

12. Romero, A.H. Reduction of Nitroarenes via Catalytic Transfer Hydrogenation Using Formic Acid as Hydrogen Source: A Comprehensive Review. *ChemistrySelect* **2020**, *5*, 13054–13075. [[CrossRef](#)]
13. Taleb, B.; Jahjah, R.; Cornu, D.; Bechelany, M.; Al Ajami, M.; Kataya, G.; Hijazi, A.; El-Dakdouki, M.H. Exploring Hydrogen Sources in Catalytic Transfer Hydrogenation: A Review of Unsaturated Compound Reduction. *Molecules* **2023**, *28*, 7541. [[CrossRef](#)] [[PubMed](#)]
14. Fang, W.; Riisager, A. Recent Advances in Heterogeneous Catalytic Transfer Hydrogenation/Hydrogenolysis for Valorization of Biomass-Derived Furanic Compounds. *Green Chem.* **2021**, *23*, 670–688. [[CrossRef](#)]
15. Eppinger, J.; Huang, K.-W. Formic Acid as a Hydrogen Energy Carrier. *ACS Energy Lett.* **2017**, *2*, 188–195. [[CrossRef](#)]
16. Enthaler, S.; von Langermann, J.; Schmidt, T. Carbon Dioxide and Formic Acid—The Couple for Environmental-Friendly Hydrogen Storage? *Energy Environ. Sci.* **2010**, *3*, 1207–1217. [[CrossRef](#)]
17. Williams, M.C. *Chapter 2—Fuel Cells*; Shekhawat, D., Spivey, J.J., Berry, D.A., Eds.; Elsevier: Amsterdam, The Netherlands, 2011; pp. 11–27, ISBN 978-0-444-53563-4.
18. Sanni, S.E.; Alaba, P.A.; Okoro, E.; Emetere, M.; Oni, B.; Agboola, O.; Ndubuisi, A.O. Strategic Examination of the Classical Catalysis of Formic Acid Decomposition for Intermittent Hydrogen Production, Storage and Supply: A Review. *Sustain. Energy Technol. Assess.* **2021**, *45*, 101078. [[CrossRef](#)]
19. Zhang, L.; Wu, W.; Jiang, Z.; Fang, T. A Review on Liquid-Phase Heterogeneous Dehydrogenation of Formic Acid: Recent Advances and Perspectives. *Chem. Pap.* **2018**, *72*, 2121–2135. [[CrossRef](#)]
20. Navlani-García, M.; Mori, K.; Salinas-Torres, D.; Kuwahara, Y.; Yamashita, H. New Approaches toward the Hydrogen Production from Formic Acid Dehydrogenation over Pd-Based Heterogeneous Catalysts. *Front. Mater.* **2019**, *6*, 44. [[CrossRef](#)]
21. Vardon, D.R.; Rorrer, N.A.; Salvachúa, D.; Settle, A.E.; Johnson, C.W.; Menart, M.J.; Cleveland, N.S.; Ciesielski, P.N.; Steirer, K.X.; Dorgan, J.R. Cis, Cis-Muconic Acid: Separation and Catalysis to Bio-Adipic Acid for Nylon-6, 6 Polymerization. *Green Chem.* **2016**, *18*, 3397–3413. [[CrossRef](#)]
22. Dong, H.; Zhao, J.; Chen, J.; Wu, Y.; Li, B. Recovery of Platinum Group Metals from Spent Catalysts: A Review. *Int. J. Miner. Process.* **2015**, *145*, 108–113. [[CrossRef](#)]
23. Liu, J.J. Advanced Electron Microscopy of Metal-Support Interactions in Supported Metal Catalysts. *ChemCatChem* **2011**, *3*, 934–948. [[CrossRef](#)]
24. Challa, S.R.; Delariva, A.T.; Hansen, T.W.; Helveg, S.; Sehested, J.; Hansen, P.L.; Garzon, F.; Datye, A.K. Relating Rates of Catalyst Sintering to the Disappearance of Individual Nanoparticles during Ostwald Ripening. *J. Am. Chem. Soc.* **2011**, *133*, 20672–20675. [[CrossRef](#)] [[PubMed](#)]
25. Zhao, T.-J.; Chen, D.; Dai, Y.-C.; Yuan, W.-K.; Holmen, A. The Effect of Graphitic Platelet Orientation on the Properties of Carbon Nanofiber Supported Pd Catalysts Prepared by Ion Exchange. *Top. Catal.* **2007**, *45*, 87–91. [[CrossRef](#)]
26. Barlocco, I.; Capelli, S.; Zanella, E.; Chen, X.; Delgado, J.J.; Roldan, A.; Dimitratos, N.; Villa, A. Synthesis of Palladium-Rhodium Bimetallic Nanoparticles for Formic Acid Dehydrogenation. *J. Energy Chem.* **2021**, *52*, 301–309. [[CrossRef](#)]
27. Sanchez, F.; Alotaibi, M.H.; Motta, D.; Chan-Thaw, C.E.; Rakotomahevitra, A.; Tabanelli, T.; Roldan, A.; Hammond, C.; He, Q.; Davies, T.; et al. Hydrogen Production from Formic Acid Decomposition in the Liquid Phase Using Pd Nanoparticles Supported on CNFs with Different Surface Properties. *Sustain. Energy Fuels* **2018**, *2*, 2705–2716. [[CrossRef](#)]
28. Wang, X.; Sun, G.; Routh, P.; Kim, D.-H.; Huang, W.; Chen, P. Heteroatom-Doped Graphene Materials: Syntheses, Properties and Applications. *Chem. Soc. Rev.* **2014**, *43*, 7067–7098. [[CrossRef](#)] [[PubMed](#)]
29. Shafeeyan, M.S.; Daud, W.M.A.W.; Houshmand, A.; Shamiri, A. A Review on Surface Modification of Activated Carbon for Carbon Dioxide Adsorption. *J. Anal. Appl. Pyrolysis* **2010**, *89*, 143–151. [[CrossRef](#)]
30. Prati, L.; Villa, A. The Art of Manufacturing Gold Catalysts. *Catalysts* **2011**, *2*, 24. [[CrossRef](#)]
31. Barlocco, I.; Bellomi, S.; Delgado, J.J.; Chen, X.; Prati, L.; Dimitratos, N.; Roldan, A.; Villa, A. Enhancing Activity, Selectivity and Stability of Palladium Catalysts in Formic Acid Decomposition: Effect of Support Functionalization. *Catal. Today* **2021**, *382*, 61–70. [[CrossRef](#)]
32. Capelli, S.; Barlocco, I.; Scesa, F.M.; Huang, X.; Wang, D.; Tessore, F.; Villa, A.; Di Michele, A.; Pirola, C. Pd–Au Bimetallic Catalysts for the Hydrogenation of Muconic Acid to Bio-Adipic Acid. *Catalysts* **2021**, *11*, 1313. [[CrossRef](#)]
33. Rosengart, A.; Pirola, C.; Capelli, S. Hydrogenation of Trans, Trans-Muconic Acid to Bio-Adipic Acid: Mechanism Identification and Kinetic Modelling. *Processes* **2020**, *8*, 929. [[CrossRef](#)]
34. Niu, W.; Draths, K.M.; Frost, J.W. Benzene-free Synthesis of Adipic Acid. *Biotechnol. Prog.* **2002**, *18*, 201–211. [[CrossRef](#)] [[PubMed](#)]
35. Capelli, S.; Rosengart, A.; Villa, A.; Citterio, A.; Di Michele, A.; Bianchi, C.L.; Prati, L.; Pirola, C. Bio-Adipic Acid Production by Catalysed Hydrogenation of Muconic Acid in Mild Operating Conditions. *Appl. Catal. B Environ.* **2017**, *218*, 220–229. [[CrossRef](#)]
36. Capelli, S.; Motta, D.; Evangelisti, C.; Dimitratos, N.; Prati, L.; Pirola, C.; Villa, A. Bio Adipic Acid Production from Sodium Muconate and Muconic Acid: A Comparison of Two Systems. *ChemCatChem* **2019**, *11*, 3075–3084. [[CrossRef](#)]
37. Capelli, S.; Motta, D.; Evangelisti, C.; Dimitratos, N.; Prati, L.; Pirola, C.; Villa, A. Effect of Carbon Support, Capping Agent Amount, and Pd NPs Size for Bio-Adipic Acid Production from Muconic Acid and Sodium Muconate. *Nanomaterials* **2020**, *10*, 505. [[CrossRef](#)] [[PubMed](#)]
38. Zanella, E.; Secundo, L.; Bellomi, S.; Vomeri, A.; Villa, A.; Pirola, C. Bio-Adipic Acid Production from Muconic Acid Hydrogenation on Palladium-Transition Metal (Ni and Zn) Bimetallic Catalysts. *Catalysts* **2023**, *13*, 486. [[CrossRef](#)]

39. Wang, X.; Li, N.; Webb, J.A.; Pfefferle, L.D.; Haller, G.L. Effect of Surface Oxygen Containing Groups on the Catalytic Activity of Multi-Walled Carbon Nanotube Supported Pt Catalyst. *Appl. Catal. B Environ.* **2010**, *101*, 21–30. [[CrossRef](#)]
40. Campisi, S.; Capelli, S.; Motta, D.; Trujillo, F.; Davies, T.; Prati, L.; Dimitratos, N.; Villa, A. Catalytic Performances of Au–Pt Nanoparticles on Phosphorous Functionalized Carbon Nanofibers towards HMF Oxidation. *C* **2018**, *4*, 48. [[CrossRef](#)]
41. Favier, I.; Pla, D.; Gómez, M. Palladium Nanoparticles in Polyols: Synthesis, Catalytic Couplings, and Hydrogenations. *Chem. Rev.* **2020**, *120*, 1146–1183. [[CrossRef](#)]

Disclaimer/Publisher’s Note: The statements, opinions and data contained in all publications are solely those of the individual author(s) and contributor(s) and not of MDPI and/or the editor(s). MDPI and/or the editor(s) disclaim responsibility for any injury to people or property resulting from any ideas, methods, instructions or products referred to in the content.